Korean J. Chem. Eng., **30**(9), 1775-1783 (2013)
DOI: 10.1007/s11814-013-0104-x

Chitosan effects on glass matrices evaluated by biomaterial. MAS-NMR and biological investigations

Hassane Oudadesse*,†, Eric Wers*, Xuang Vuong Bui*, Claire Roiland*, Bruno Bureau*, Imane Akhiyat*,, Amany Mostafa*,***, Hassan Chaair**, Hicham Benhayoune****, Joel Fauré****, and Pascal Pellen-Mussi***

*University of Rennes 1, SCR, UMR CNRS 6226, 263 av. du Général Leclerc, 35042 Rennes, France
**Université Hassan II, Faculté des Sciences et Techniques de Mohammedia (FSTM), Maroc
***Biomaterilas Department, National Research Centre (NRC), 12622 Dokki, Cairo, Egypt
****LISM-URCA, 21 rue Clément Ader, BP 138, 51685, Reims Cedex 02, France
(*Received 22 March 2013 • accepted 12 June 2013*)

Abstract−Bioactive glass 46S6 and biodegradable therapeutic polymer (Chitosan: CH) have been elaborated to form 46S6-CH composite by freeze-drying process. The kinetics of chemical reactivity and bioactivity at the surface were investigated by using physicochemical techniques, particularly solid-state MAS-NMR. Immortalized cell line used to construct multicellular spheroids was employed as three-dimensional (3D) cell cultures for *in vitro* studies. Obtained results showed a novel structure of the composite; the chemical treatment (ultrasound, magnetic stirring, freeze drying process and lyophilization) led the bioactive glass particles to be loaded in the chitosan-based materials. ^{29}Si and ^{31}P MAS-NMR results showed the emergence of two new species, Q_{Si}^3(OH) and Q_{Si}^4, which are characteristic of the vitreous network dissolution in simulated body fluid (SBF). MAS-NMR also confirmed the formation of amorphous calcium phosphate (ACP) at the surface of the initial 46S6-CH. Three-dimensional (3D) cell cultures highlighted the effect of chitosan, where the cell viability reached up to 78% in 46S6-CH composite and up to 67% in 46S6. The association of (CH) and bioactive glass (BG) matrix promotes a highly significant bioactivity, demonstrating surface bone formation and satisfactory behavior in biological environment.

Key words: Bioactive Glass, Chitosan, Composite, Bioactivity, Hydroxyapatite, ^{31}P MAS NMR, ^{29}Si MAS NMR, Immortalized Cell, 3D Cells Viability

INTRODUCTION

Bioactive glasses are a group of reactive surface glass-ceramic biomaterials used as implant materials in the human body to repair and replace a diseased or damaged bone. Their bioactivity is based on the ability to form a biological apatite layer when they are immersed in a physiological solution or implanted in human body. The formation of apatite layer promotes the adhesion of bone tissues and permits an intimate bone-bonding with the implants. Consequently, the bone architecture is repaired and reconstructed [1,2].

The composites based on biodegradable polymers and bioactive ceramics have attracted much attention for applications in bone reconstruction and repairing because of their biological and physicochemical advantages. Some polymers have been used for this purpose, such as synthetic polymers like polylactic acid (PLA), polyglycolic acid (PGA), poly caprolactone, polylactic-co-glycolic acid (PLGA) and natural polymers like gelatin, alginate, collagen, chitin and chitosan [3-7].

Chitosan is a low cost natural biodegradable polymer that has special physiological properties. Chitosan has been obtained by partial deacetylation of chitin. It is considered as a suitable functional material for biomedical applications because of its non-toxic character, good biocompatibility, non-antigenicity, anti-tumor activity and protein adsorption properties. It promotes cell adhesion and migration, enhances wound healing, and is biodegradable at a rate in accordance with controlled factors such as degree of deacetylation, molecular weight, and crystallinity [8-11].

Bioactive ceramic such as bioactive glass is well known for its use as a bone implant material that is characterized by being brittle. Chitosan, on the other hand, is tough and flexible, but lacks sufficient strength to be used alone in load bearing applications. A composite constituting these two biomaterials has better mechanical properties that can support healing tissues. Several biodegradable polymer/bioactive ceramic composites possess a good bioactivity, which is illustrated by rapid bone repair and a good osteoinductivity expressed by the enhancement of bone cell growth and differentiation [12-15].

In this work, the elaboration of 46S6 glass by the melting method, as well as the association of bioactive glass particles and chitosan polymer to synthesize the 46S6-CH composite was carried out. In addition, the *in vitro* kinetics of chemical reactivity and bioactivity of these two biomaterials were investigated with main focus on using the nuclear magnetic resonance spectroscopy. Cell biocompatibility assays were also performed by using an immortalized cell line to construct multi cellular spheroids employed as three-dimensional (3D) cell cultures for *in vitro* studies (Osteoblasts $SaOS_2$). The following was evaluated: 1) the new structure of the synthesized biomaterial, 2) kinetics of the chemically reactivity of 46S6 glass as compared to its pure counterpart, and 3) cells viability by using origi-

†To whom correspondence should be addressed.
E-mail: hassane.oudadesse@univ-rennes1.fr

nal 3D cell cultures.

MATERIALS AND METHODS

1. Elaboration of 46S6 Glass

Bioactive glass with the chemical composition of 46 wt% SiO_2, 24 wt% CaO, 24 wt% Na_2O and 6 wt% P_2O_5 was prepared by the melting method according to the heating regime previously reported in our work [16]. The starting materials, calcium silicate ($CaSiO_3$), sodium Meta silicate (Na_2SiO_3) and sodium phosphate ($NaPO_3$), were weighed and mixed homogeneously. The mixture was then heated in a platinum crucible according to the following steps. First, the temperature was ramped to 900 ºC and then kept at 900 ºC for 1 hour to decompose the chemical constituents. Afterwards, the temperature was raised and kept at 1300 ºC for 3 hours to melt the reactive mixture. The melted bioactive glass was then poured into preheated brass moulds and annealed for 4 hours at the glass transition temperature (about 536 ºC) to remove the residual mechanical stress. After cooling to room temperature, the bulk glasses were ground into powder and sieved to obtain bioactive glass particles with size less than 40 μm.

2. Elaboration of 46S6 Bioactive Glass/Chitosan Composite

The 46S6-CH composite containing 17 wt% of chitosan polymer was elaborated following several steps (Fig. 1). The content of chitosan biopolymer was fixed following several tests (12 wt%, 15 wt%, 17 wt%, 19 wt% and 21 wt%). XRD, FTIR, SEM and EDAX preliminary assays showed that the optimum concentration was 17 wt% of chitosan and 83% of glass [17,18]. First, chitosan polymer is a natural biodegradable polymer that is obtained by partial deacetylation of chitin, which is extracted from crustacean. Chitosan with medium molecular weight MMW: 480,000 Da and degree of deacetylation 85% was dissolved in a 1 wt% acetic acid aqueous solution. This solution was stirred and filtered to obtain a homogeneous viscous polymer solution. During this time, the bioactive glass (BG) suspension was prepared by ultrasonication of the glass microparticles in 2 ml of 1 wt% acetic acid for 30 min. Then, the prepared BG suspension was suspended into chitosan solution and stirred at 1,200 rpm for 2 hours to obtain a homogeneous mixture. After eliminating surplus solution, the mixture of 46S6-CH was immersed in

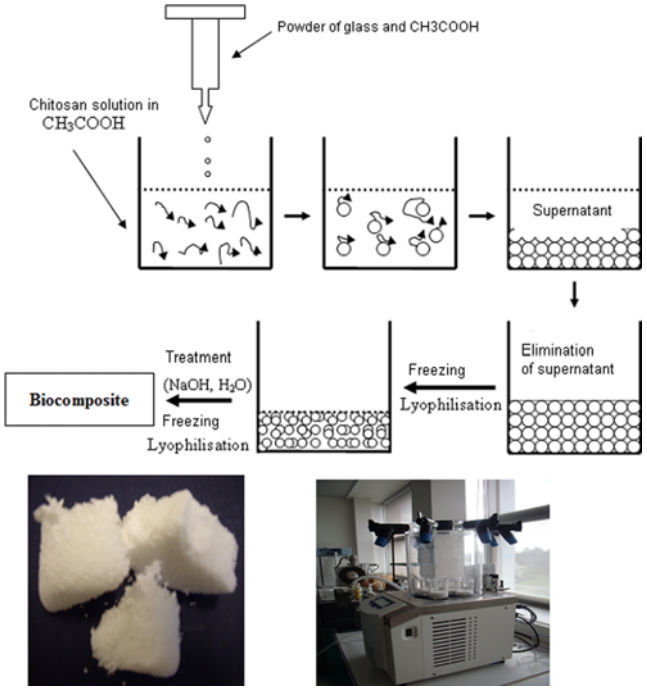

Fig. 1. Composite glass and chitosan elaboration 46S6-CH.

10% NaOH solution for two hours and washed several times with distilled water to neutralize the residues of acetic acid. Finally, the composite particles were frozen by liquid azotes for 30 minutes and transferred into a freeze-dryer (Christ Alpha 1-2 LD plus, version 1.26) at −60 ºC, 1 mbar for 24 hours to totally remove the solvent. Scanning electron microscopy was performed to highlight the morphology of the obtained composite (Fig. 2).

3. *In Vitro* Immersions in SBF

The *in vitro* study of 46S6 glass and 46S6-CH composite was done by soaking 100 mg of material samples into 200 ml of simulated body fluid (SBF) with pH and mineral composition similar to that of human blood plasma. The SBF solution was prepared by dissolving the chemical reagent of NaCl, $NaHCO_3$, KCl, $K_2HPO_4 \cdot 3H_2O$, $MgCl_2 \cdot 6H_2O$ and $CaCl_2$ into deionized water and buffering

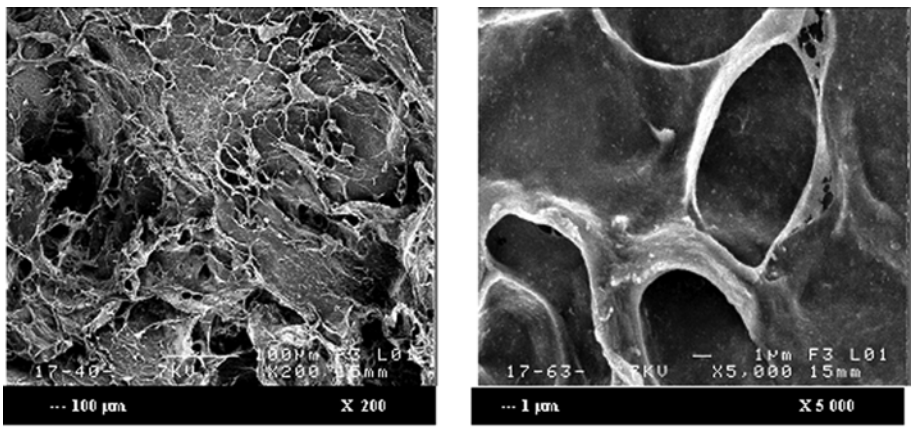

Fig. 2. SEM graphs of composite 46S6-CH.

Table 1. Concentrations of the SBF solution, 10^{-3} mol·L^{-1}

Ions	Na^+	K^+	Ca^{2+}	Mg^{2+}	Cl^-	HCO_3^-	HPO_4^{2-}
SBF	142.0	5.0	2.5	1.5	148.8	4.2	1.0
Plasma	142.0	5.0	2.5	1.5	103.0	27.0	1.0

with $(CH_2OH)_3CNH_2$ and HCl 6 N to obtain a pH value of 7.4 according to Kokubo's technique [19]. The ionic concentrations of this solution are shown in Table 1. The powder samples were immersed in SBF solution and maintained at body temperature (37 °C) under controlled agitation of 50 rpm for 1, 3, 7, and 15 days.

4. Immortalized Cell Line - 2D and 3D Cell Cultures

Human osteosarcoma cell line $SaOS_2$ was plated into 75 cm^2 culture flasks in culture medium, supplemented with 10% foetal calf serum, 15 mM HEPES ((4-(2-hydroxyethyl)-1-piperazineethanesulfonic acid) buffer, 2 mM L-Glutamine, 100 UI·mL^{-1} penicillin and 100 μg·mL^{-1} streptomycin at 37 °C in a humidified incubator of 5% (v/v) CO_2. After reaching approximately 80% confluency, cells were harvested and subcultured by rinsing the cell layer with 0.1% (w/v) trypsin and 0.02% (w/v) EDTA followed by a rapid dilution in BM. Studies were carried out for 2D and 3D cell culture.

2D cell culture: $SaOS_2$ cells were harvested and plated in 96-well micro plates with 200 μL of culture medium. The initial concentrations were of 2.5×10^4 cells·mL^{-1} for three days assays and of 1×10^4 cells·mL^{-1} for six days assays. Micro plates were incubated for 24 h to allow adhesion of the monolayer cultures before the contact with conditioned media.

3D cell culture: 96-well micro plates were firstly coated with 50 μL of a 1.5% agarose gel. Then, $SaOS_2$ cells were harvested and deposited in coated micro plates with 200 μL of medium. The initial concentration is of 1×10^4 cells·mL^{-1}. Before the contact with conditioned media, micro plates were incubated four days to allow spheroids formation before the contact with conditioned media.

Culture medium of the association 46S6-CH composite was obtained by soaking 0.2 g of 46S6-CH particles in 100 mL of DMEM. Concentration of particles of pure glass 46S6 and pure chitosan was, respectively, 0.16% (p/V) and 0.04% (p/V). After 24 h of incubation at 37 °C in a humidified incubator of 5% (v/v) CO_2, the culture medium was filtered through 0.2 μm sterile filter. Filtered extracts were supplemented with 10% (v/v) FCS, 2 mM L-Glutamine and 25 mM HEPES ((4-(2-hydroxyethyl)-1-piperazineethanesulfonic acid) buffer.

Cell viabilities (Osteoblast cells: $SaOS_2$) were evaluated with culturing times of 3 and 6 days in pure glass, in pure chitosan, and in composite 46S6-CH to highlight the chitosan effect.

5. Physicochemical Characterizations

Physicochemical characterizations were performed on the layer formed on the surface of glasses after soaking in SBF solution. This layer was removed by scraping. X-ray diffraction measurements were realized on a Bruker D8 Advance diffractometer. Powder samples were mixed homogeneously with cyclohexane and dropped on the surfaces of plastic tablets. Then, these tablets were dried to remove the solvent and were then introduced into a diffractometer. The X-ray diffraction (XRD) data were acquired in the range of 10-70° (2θ) with a scanning speed of 1°/min. Nuclear magnetic resonance (MAS-NMR) method to investigate the kinetics of chemical reactivity and bioactivity of 46S6 glass and 46S6-CH composite after the *in vitro* assays was employed [17]. The ^{29}Si and ^{31}P MAS-NMR spectra were measured on a Bruker Avance 300 spectrometer (7T). Material samples were packed in zirconium rotors with a diameter of 2.5 mm, and spun at the magic angle of 54.7° with a spinning frequency of 15 MHz. The deconvolution of the MAS-NMR spectra was performed on the dmfit2010 software [20].

RESULTS AND DISCUSSION

1. Physicochemical Behaviour of Biomaterials Before and After Assay in SBF Solution

1-1. X-ray Diffraction Characterization

XRD diagrams of the surface of 46S6 glass before and after soaking in SBF were studied in our previous work [17]. The XRD diagrams of the surface of initial glass do not show any evidence of crystalline phase, which confirms the amorphous character of glass. A diffraction halo with center at 32.5° (2θ) characteristic of the diffusion phenomena in amorphous materials can be observed. The XRD results after seven days shows two characteristic peaks of hydroxyapatite at 26 and 32°. They correspond, respectively, to the (002) and (211) reflection planes in the structure of hydroxyapatite crystals. These two apatite's peaks are found to be more intensive after 15 days of immersion. On the other hand, four other small peaks at 40, 46.7, 50 and 53° are also exhibited [17]. They are, respectively, attributed to the (310), (222), (213) and (004) reflection planes in the crystallographic system of the hydroxyapatite. This result indicates that the amount and the crystalline quality of apatite layer formed on the surface of 46S6 glass compound increases with time of soaking in SBF solution. The X-ray diffractogram of the initial 46S6-CH composite exhibited one characteristic peak of chitosan (CH) at about 20° (2θ). This illustrates the presence of chitosan in the structure of synthetic composite. The diffraction halo characteristic of the amorphous structure of bioactive glass is shifted to the left and seems more pointed. The shift and appearance of a new peak at 29° manifests the chemical interactions occurring between glass and chitosan polymer in the process of composite elaboration, which induced the changes in amorphous structure of glass. After three days of soaking in SBF solution, the characteristic peaks of hydroxyapatite clearly emerged in the X-ray diagram of 46S6-CH composite. This illustrates the rapid rate of formation of hydroxyapatite layer on the surface of 46S6-CH composite in comparison with pure 46S6 glass. With the increase in the immersion time, the intensities of the characteristic peaks of hydroxyapatite phase became more visible. After seven and 15 days of immersion, the diffractogram of 46S6-CH composite shows all of the characteristic peaks of hydroxyapatite crystals [17]. It is recognized that the hydroxyapatite peaks on the diffractogram of 46S6-CH composite are clearer than those of 46S6 glass. This confirms the proper crystallization of the apatite layer on the surface of the synthetic composite after *in vitro* assay.

1-2. ^{31}P MAS-NMR Characterization

Fig. 3 presents the ^{31}P MAS-NMR spectra of 46S6 glass before and after soaking in SBF solution. Table 2 lists the data of the different components after the spectral deconvolutions. The ^{31}P MAS-NMR spectrum of the initial 46S6 glass shows only one resonance (Fig. 3(a)). Its chemical shift (δ) and full width at half-maximum (fwhm) are characteristic of the phosphate tetrahedral PO_4^{3-} without

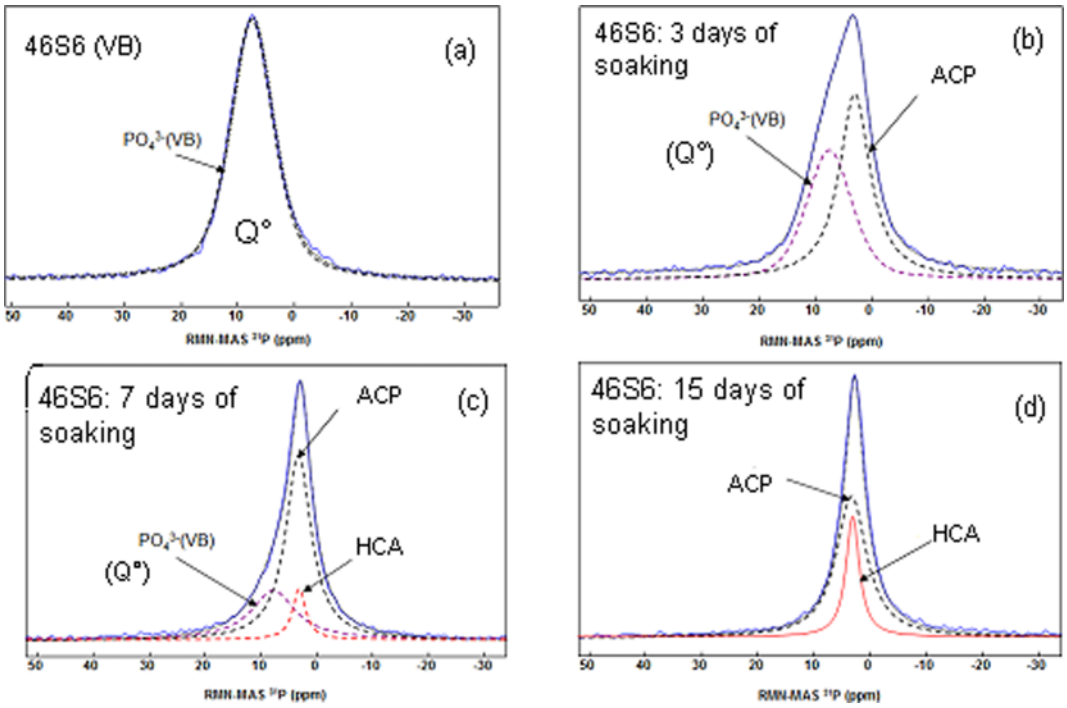

Fig. 3. ^{31}P MAS-NMR spectra of 46S6 glass: (a) initial 46S6 glass, (b) after 3 days, (c) after 7 days and (d) after 15 days of soaking in SBF solution.

Table 2. ^{31}P MAS-NMR data of 46S6 glass before and after soaking in SBF solution

Soaking time	^{31}P MAS-NMR data of 46S6 glass								
0 Day	Q_P^0								
	δ (ppm)	%	fwhm (ppm)						
	7.57	100	9.19						
3 Days	Q_P^0			ACP					
	δ (ppm)	%	fwhm (ppm)	δ (ppm)	%	fwhm (ppm)			
	7.54	45.17	9.52	3.01	54.83	6.65			
7 Days	Q_P^0			ACP			HCA		
	δ (ppm)	%	fwhm (ppm)	δ (ppm)	%	fwhm (ppm)	δ (ppm)	%	fwhm (ppm)
	7.61	28.43	9.56	3.10	62.92	5.60	2.96	8.65	2.80
15 Days				ACP			HCA		
				δ (ppm)	%	fwhm (ppm)	δ (ppm)	%	fwhm (ppm)
				3.13	72.20	6.61	2.94	27.80	2.81

bridging oxygen, named as orthophosphate [20-22,33]. Q_P^0 code was used to denote the tetrahedrons PO_4^{3-} in the initial 46S6 glass and hence differentiate between it and other phosphorus species in the same orthophosphate environment. After three days of immersion in SBF solution, the quantity of Q_P^0 was shown to decrease strongly due to the release of phosphorus from the glassy network under the active effect of the SBF solution. On the other hand, a new resonance is observed as shown in (Fig. 3(b)). This resonance is assigned to amorphous calcium phosphate (ACP) as reported by previous workers [23-26,27]; where the synthetic amorphous calcium phosphate (ACP) revealed a chemical shift (δ) around 3 ppm and a full width at half-maximum (fwhm) in the range 4.4-6.9 ppm. This result is in agreement with the previous analyses by X-ray diffraction [17], where the 46S6 glass was still amorphous material after three days of immersion. It is also consistent with the bioactivity mechanism of bioactive glass, described by Hench et al. [1,2], where there is the deposit of the Ca^{2+} and PO_4^{3-} ions to form an amorphous calcium phosphate (ACP) on the surface of glass after soaking in SBF solution. After seven days of immersion, the amount of Q_P^0 decreased continuously and strongly while an increase of ACP and an appearance of a new resonance were observed (Fig. 3(c)). The new resonance has the δ and fwhm characteristic to hydroxyl carbonated apatite (HCA), and hence is in agreement with the previous studies [26-28] where the hydroxyl carbonated apatite obtained after

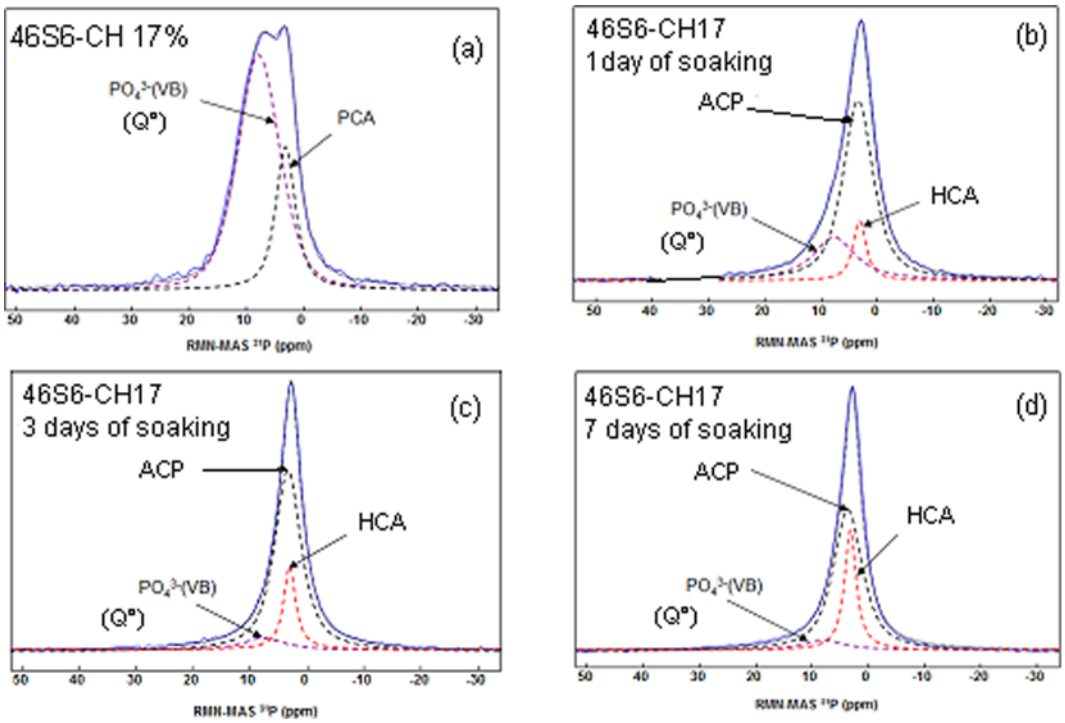

Fig. 4. ^{31}P MAS-NMR spectra of 46S6-CH composite: (a) initial 46S6-CH composite, (b) after 1 day (c) after 3 days and (d) after 7 days of soaking in SBF solution.

Table 3. ^{31}P MAS-NMR data of 46S6-CH composite before and after soaking in SBF solution

Soaking time	^{31}P MAS-NMR data of 46S6-CH composite								
	Q_P^0			ACP					
0 Day	δ (ppm)	%	fwhm (ppm)	δ (ppm)	%	fwhm (ppm)			
	7.67	75.68	8.86	2.98	24.32	4.41			
	Q_P^0			ACP			HCA		
1 Days	δ (ppm)	%	fwhm (ppm)	δ (ppm)	%	fwhm (ppm)	δ (ppm)	%	fwhm (ppm)
	7.65	24.18	9.13	3.22	65.53	6.40	2.96	10.30	2.78
	Q_P^0			ACP			HCA		
3 Days	δ (ppm)	%	fwhm (ppm)	δ (ppm)	%	fwhm (ppm)	δ (ppm)	%	fwhm (ppm)
	7.55	8.38	9.06	3.20	74.87	5.62	2.89	16.75	2.51
	Q_P^0			ACP			HCA		
7 Days	δ (ppm)	%	fwhm (ppm)	δ (ppm)	%	fwhm (ppm)	δ (ppm)	%	fwhm (ppm)
	7.67	6.87	8.76	3.43	67.73	6.24	2.96	25.40	2.52

in vitro assays exhibited a chemical shift about 3 ppm and a full width at half-maximum from 2 to 2.8 ppm. This result again agrees well with the XRD analyses, where the 46S6 glass revealed two characteristic peaks of hydroxyapatite after seven days of soaking in SBF solution. It also accords with the bioactivity mechanism of bioactive glass [1,2], in which the amorphous calcium phosphate (ACP) evolves into crystalline hydroxyl carbonated apatite (HCA) with the increase of immersion time. After 15 days of immersion in SBF solution, the Q_P^0 species clearly disappeared while the HCA component increased quickly (Fig. 3(d)). The disappearance of Q_P^0 units confirms their complete migration out of the glassy network into the SBF solution. The increase of HCA quantity corresponds to the progressive crystallization of the amorphous calcium phosphate (ACP) to form the hydroxyl carbonated apatite crystals (HCA) [27].

Fig. 4 shows the ^{31}P MAS-NMR spectra of 46S6-CH composite before and after soaking in SBF solution. The spectral data of the deconvoluting components are presented in Table 3. Before immersion in SBF solution, the ^{31}P MAS-NMR spectrum of 46S6-CH composite shows two resonances as shown in Fig. 4(a). They are all characteristic of the orthophosphate environment. The first resonance has the δ and fwhm assigned to the units Q_P^0 as observed in

the initial 46S6 glass spectrum. The second resonance possesses the δ and fwhm values characteristic of an amorphous calcium phosphate (ACP) [23-28]. The presence of ACP phase in the initial composite shows the effect of chitosan addition on the structure of bioactive glass. This result may be consistent with the previous observation for the XRD diagram of synthetic composite where the diffraction halo characteristic of the amorphous structure of bioactive glass is shifted to the left and seems more pointed. The synthesis of 46S6-CH composite passes several steps as follows: immersion of 46S6 glass particles in the chitosan solution, mixing using the magnetic stirring, neutralizing in NaOH, washing in distilled water and freeze-dried. The interactions between glass and chitosan in these processes may cause the transfers of the PO_4^{3-}, Ca^{2+} ions present in the glassy matrix, which leads to the deposition of an amorphous calcium phosphate (ACP) in the structure of synthetic composite. The quantity of Q_P^0 units diminishes quickly after one day of soaking. This decrease is characteristic of the release of phosphorus from the 46S6-CH composite under the active effect of the SBF solution. Furthermore, an increase of ACP amount and the emergence of hydroxyl carbonated apatite (HCA) are observed as shown in (Fig. 4(b)). This result confirms the rapid formation of HCA phase on the surface of composite after *in vitro* assays. The HCA amount increases gradually with time of immersion (Fig. 4(c), (d)). After seven days, the quantity of hydroxyl carbonated apatite formed on the surface of 46S6-CH composite is approximately equal to the one pertaining to 46S6 glass after 15 days of soaking. This result confirms with a precise assay the high bioactivity of 46S6-CH composite in comparison to pure 46S6 glass [27].

1-3. ^{29}Si MAS-NMR Characterization

Fig. 5 shows the ^{29}Si MAS-NMR spectra of 46S6 glass before and after soaking in SBF solution, while Table 4 presents the relevant data pertaining to the different species after the spectral deconvolutions. The spectrum of glass after one day is not shown as it is similar to the one describing soaking after three days. The deconvoluting spectrum of the initial 46S6 glass shows two resonances. The first chemical shift is assigned to Q_{Si}^2 species (SiO_4 tetrahedron is linked into the vitreous network via two bridging oxygen). The second chemical shift is characteristic of Q_{Si}^3 species (SiO_4 tetrahedron is linked into the vitreous network via three bridging oxygen) [20-22,33]. The chemical neutrality around the non-bridging oxygen of Q_{Si}^3 tetrahedral is respected by the preferential presence of Na^+ cations, and is shown as $Si(OSi)_3(O\ldots Na)$. The non-bridging oxygens of Q_{Si}^2 species are rather combined with Ca^{2+} cations and Na^+ remaining cations. These two combinations could be expressed as $Si(OSi)_2(O_2\ldots Ca)$ and $Si(OSi)_2(O\ldots Na)_2$ [19,20]. The ^{29}Si MAS-NMR spectrum of 46S6 glass shows some changes as a function of soaking time in SBF solution. This characterizes the structural modification of the vitreous matrix due to the chemical reaction between glass and SBF solution. In fact, the quantities of Q_{Si}^2 and Q_{Si}^3 species decrease gradually while two new components $Q_{Si}^3(OH)$ and Q_{Si}^4 emerged on the spectrum of 46S6 glass after *in vitro* assays. The $Q_{Si}^3(OH)$ characterizes the tetrahedral environment of Si with three bridging oxygen and one hydroxyl group [29-30]. The Q_{Si}^4 is characteristic of the silicon in tetrahedral environment with four bridging oxygen. This silicon environment corresponds to pure silica (SiO_2) [31-34]. The emergence of two new components $Q_{Si}^3(OH)$ and Q_{Si}^4 is witness to the dissolution of glassy network. These obtained results are relevant to the progressive chemical reactions between bioactive glass and the physiological fluid SBF, discovered by Hench et al. [1,2]. The first is the dealkalization process through the inter diffusion/ion-exchange of Na^+, Ca^{2+} out of the glass and H_3O^+ into the glass to form the Si-OH groups. Then, the reactions of the breaking of Si-O-Si bridging links occur at the interface glass/liquid SBF, which leads to the loss of soluble silica $Si(OH)_4$. The pursuit of the two above reactions is the condensation and repolymerization of surface silanols to form SiO_2-rich layer, expressed by the increase of species $Q_{Si}^3(OH)$ and Q_{Si}^4. These key reactions are illustrated below.

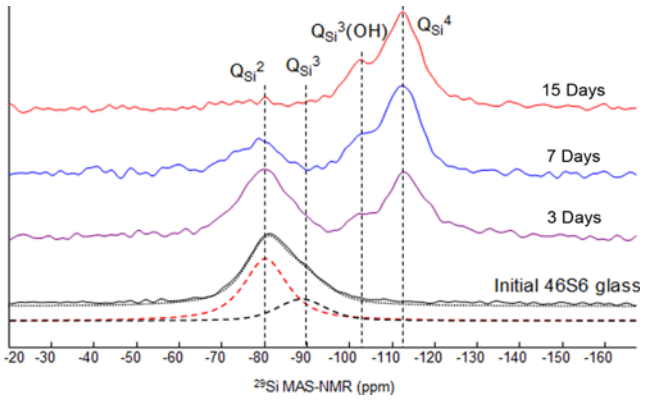

Fig. 5. ^{29}Si MAS NMR spectra of 46S6 glass before and after soaking in SBF solution.

After 15 days of immersion in SBF solution, all species of Q_{Si}^2 and Q_{Si}^3 disappeared. This confirms the termination of the chemical reactions 1, 2 and 3. The ^{29}Si MAS-NMR spectrum of 46S6 glass shows only two species: $Q_{Si}^3(OH)$ and Q_{Si}^4. Their percentages as shown in Table 4 confirm the formation of a SiO_2-rich gel layer on the surface of glass after 15 days of immersion.

Fig. 6 shows the ^{29}Si MAS-NMR spectra of 46S6-CH composite before and after soaking in SBF solution. Percentage contribution

Table 4. ^{29}Si MAS-NMR data of 46S6 glass before and after soaking in SBF solution

Soaking time	^{29}Si MAS-NMR data of 46S6 glass									
	Q_{Si}^2		Q_{Si}^3		$Q_{Si}^2+Q_{Si}^3$	$Q_{Si}^3(OH)$		Q_{Si}^4		$Q_{Si}^3(OH)+Q_{Si}^4$ (%)
	δ (ppm)	%	δ (ppm)	%		δ (ppm)	%	δ (ppm)	%	
0 Day	−80.3	79.5	−89.2	20.5	100		0		0	0
3 Days	−80.0	56.4		0	56.4	−102.5	6.1	−113.2	37.5	43.6
7 Days	−79.1	28.0		0	28.0	−102.3	17.0	−112.5	55.0	72.0
15 Days		0		0	0	−102.0	24.7	−112.5	75.3	100

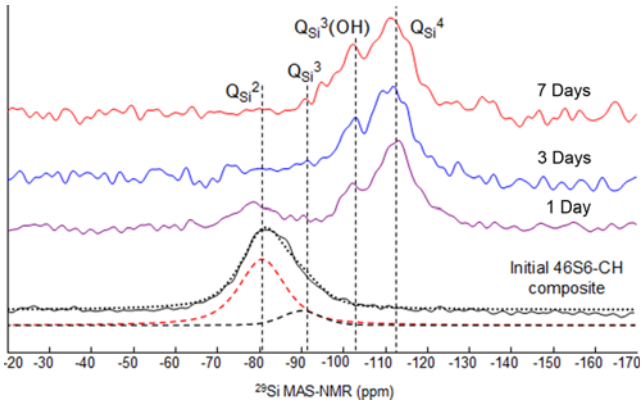

Fig. 6. ^{29}Si MAS NMR spectra of 46S6-CH composite before and after soaking in SBF solution.

of the different species after the spectral deconvolutions is presented in Table 4. A spectrum of the composite after 15 days is not presented here because it did not change much compared to the one pertaining to soaking after seven days. The deconvoluting spectrum of the initial 46S6-CH composite also shows two resonances attributed, respectively, to Q_{Si}^2 and Q_{Si}^3 units as observed in the initial 46S6 glass, but the quantity of Q_{Si}^2 is more than the one for the initial 46S6 glass. Thus, there is a transfer from Q_{Si}^3 species to Q_{Si}^2 species in the composition of 46S6-CH composite. This highlights the effect of chitosan addition on the pure 46S6 glass structural model It could be deduced that chitosan breaks one bridging link Si-O-Si in Q_{Si}^3 tetrahedral to form Q_{Si}^2 tetrahedral. Because of the breaking of links, the chitosan can create intimate links to the vitreous matrix of 46S6 glass. After immersion in SBF liquid, the dissolution of glassy network in 46S6-CH composite is faster than that in 46S6 glass. The ^{29}Si MAS-NMR spectrum of 46S6-CH composite significantly reveals two new resonances attributed, respectively, to species Q_{Si}^3(OH) and Q_{Si}^4 after the first day of immersion. After three days of immersion, the species Q_{Si}^2 and Q_{Si}^3 completely disappeared. The ^{29}Si MAS-NMR spectrum of 46S6-CH composite shows two components, Q_{Si}^3(OH) and Q_{Si}^4. Their percentages as shown in Table 5 are nearly equal to the ones of 46S6 glass after 15 days of immersion. This indicates the rapid dissolution of glassy network of 46S6-CH composite in comparison to 46S6 glass after *in vitro* assay.

1-3-1. Specific Surface Area and Porosity

The graphical form of the BET isothermal line presented in our previous work [17] exhibits a type IV isotherm, typical of a mesoporous structure. The specific surface areas of bioactive glass 46S6 and chitosan are 0.90 and 0.70 (m^2/g), respectively; however, the specific surface area of biocomposite 46S6-CH is 14.9 (m^2/g). Thus, the surface area of the biocomposite is too high in comparison with bioactive glass and chitosan polymer. In addition, the percentage of porosity of biocomposite is determined by the liquid displacement method. Scanning electron microscopy (SEM) images highlight the important porosity of composite 46S6-CH as shown in Fig. 2.

This experimental value is of 80%. The obtained results highlight the large specific surface area and the high void ratio of biocomposite 46S6-CH in comparison with bioactive glass and chitosan polymer. The mentioned physicochemical characteristics of surface area and porosity contribute to and have an effect on the cell viability of the prepared composite. Various surface treatments with inorganic hydrophilic silica and/or organic chitosan have been proven to influence cell growth along pore walls. Therefore, the increasing of surface area and porosity has an impact on the cell growth as they facilitate interactions with cells and promote the placement of cells in the pores and consequently their proliferation.

3-2. Immortalized Cell Line - 2D and 3D Cell Cultures

3-2-1. *In Vitro* Immersions

2D cell culture: The cell viabilities in the presence of conditioned media of 46S6 glass and 46S6-CH composite are presented in Fig. 7. After three days of culturing, the $SaOS_2$ cell viabilities reached up to 116.4% for 46S6-CH composite, whereas only up to 111.8% was achieved for pure 46S6 glass with particle size of 50 μm. Six days after soaking in SBF, the $SaOS_2$ cell viabilities reached up to 107.4% for 46S6-CH composite, whereas only up to 99.1% was achieved for pure 46S6 glass as shown in Fig. 7.

In our previous work [35,36] we demonstrated that a particle size of about 50 μm of bioactive glass offers good cell viability (100%) when diluted at 10% in culture medium; however, bioactive glass with particle size of 500% diluted at 10% in culture medium at 10%

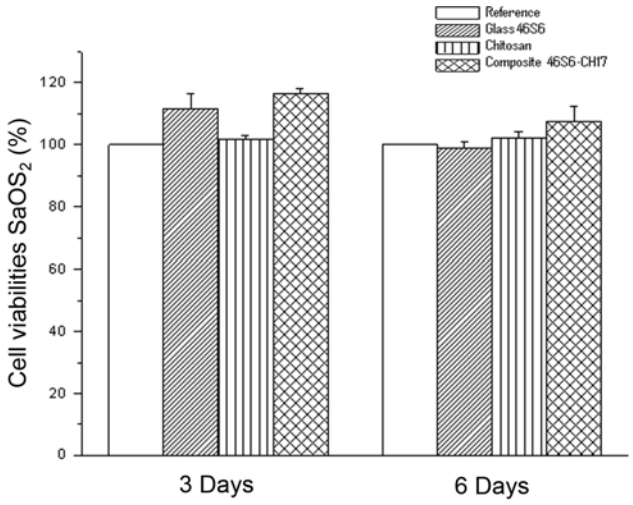

Fig. 7. 2D cell culture: $SaOS_2$ cell viabilities after 3 and 6 days of soaking in SBF.

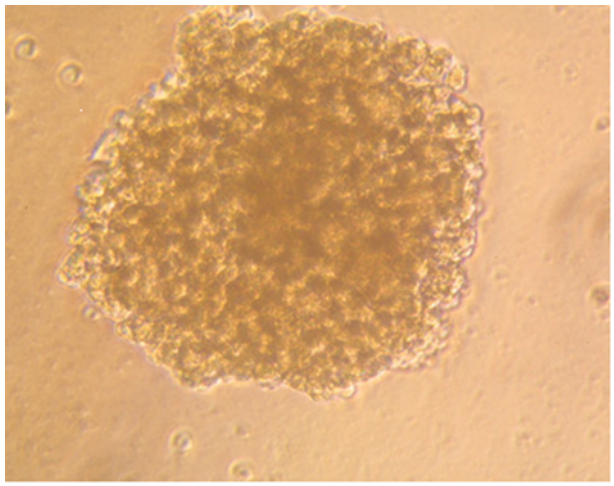

Fig. 8. 3D cell culture: Multicellular spheroids elaboration through $SaOS_2$ cells.

offers only 89% of cell viability.

3D cell culture: At four days, the diameter of spheroids was measured. Obtained results show that initial seeding of 2000 cells of $SaOS_2$ osteoblasts presents spheroids with a diameter between 180 and 250 µm. Fig. 8 shows the multi cellular spheroids of $SaOS_2$ cells. The cellular growth within spheroids has been confirmed by measurements of 3D-BM-unconditioned spheroids over a period of 36 days [35,36].

It is recognized that the decrease rate of cell viabilities for 46S6 glass is faster than that for 46S6-CH composite. This highlights the effect of CH addition on compatibility of composite with culturing cells. These results confirm that the cell compatibility on 46S6-CH composite is better than the one on 46S6 glass. In summary, the 46S6-CH composite shows better cell viability and absence of toxicity relative to the control and the 46S6 glass. This result may find potential applications for bone repair and tissue engineering.

CONCLUSION

Comparison of the behavior of pure glass and composite glass-chitosan highlighted the effects of chitosan on the kinetic of chemical reactivity and bioactivity. Solid-state ^{29}Si and ^{31}P MAS-NMR coupled to XRD and FT-IR give important information of these two biomaterials after soaking in SBF solution. Solid-state ^{29}Si and ^{31}P MAS-NMR proved to be a very sensitive technique for elucidating the *in vitro* chemical reactivity and bioactivity of 46S6 glass and 46S6-CH composite. This technique has been used to investigate the composite based on glass and chitosan. Solid-state ^{31}P MAS-NMR highlighted the formation of an amorphous calcium phosphate (ACP) in the composition of initial 46S6-CH composite. When combined with X-ray diffraction, it confirmed the high bioactivity of 46S6-CH composite. Solid-state ^{29}Si MAS-NMR showed the emergence of two new components $Q_{Si}^3(OH)$ and Q_{Si}^4, which characterizes the dissolution of the vitreous network of 46S6 glass and 46S6-CH composite after *in vitro* assays. It also highlighted the rapid dissolution of glassy network in 46S6-CH composite in comparison to 46S6 glass. The deposition of Calcium phosphate allows 46S6-CH to form a chemical bond with the bone tissue. The advantages of the novel structure of the composite 46S6-CH lead to the acceleration of the chemical reactivity and then the bioactivity compared to pure glass 46S6. Also, the antiosteoporotic property of biopolymer is well known. Furthermore, chitosan can serve as therapeutic biopolymer for the treatment of osteoporosis; this study will be evaluated *in vivo* in our future work. However, the two biomaterials could be adapted for different applications in the biomedical field.

The bioconsolidation at the interface implant/bone depends widely on some factors such as the age, gender, location site and bony metabolism. Concerning a young body, the intense metabolism activities favor the application and the use of the 46S6-CH composite because of its rapid formation of biological apatite, responsible for a good and fast bioconsolidation. Surgeons have more possibilities for the use of pure bioactive glass or composite glass-chitosan according to the mentioned parameters.

ACKNOWLEDGEMENT

Authors would like to thank the CRMPO centre of University of Rennes 1, Joseph Le Lannic, Isabelle Peron and Francis Gouttefangeas from The CMEBA centre of University of Rennes 1 for helping with the NMR, SEM and EDS devices and measurements.

REFERENCES

1. L. L. Hench, R. J. Splinter, W. C. Allen and T. K. Greenlee, *J. Biomed. Mater. Res.*, 5, 117 (1971).
2. L. L. Hench, *J. Sci. Mater: Mater. Med.*, **17**, 967 (2006).
3. J. Rich, T. Jaakkola, T. Tirri, T. Narhi, A. Yli-Urpo and C. Seppala, *J. Biomater.*, **23**, 2143 (2002).
4. D. Walsh, T. Furuzono and A. Tanaka, *J. Biomater.*, **22**, 1205 (2001).
5. J. Devin, M. Attawia and C. Laurencin, *J. Sci. Biomater. Polym. Edn.*, **7**, 661 (1996).
6. I. B. Leonor, E. T. Baran, M. Kawashita, R. L. Reis, T. Kokubo and T. Nakamura, *Acta Biomater.*, **4**, 1349 (2008).
7. W. W. Thein-Han and R. D. K. Misra, *Acta Biomater.*, **5**, 1182 (2008).
8. G. Brandenberg, L. G. Leibrock, R. Shuman and W. G. Malette, *Neurosur.*, **15**, 9 (1984).
9. R. A. Muzzarelli, F. Tanfani, M. Emanuelli, D. P. Pace and E. Chiumzzi, *Res. Carbohyd.*, **126**, 225 (1984).
10. S. Hirano and Y. Yagi, *Res. Carbohyd.*, **8**, 103 (1980).
11. L. Jiang, Y. Li, X. Wang, L. Zhang, J. Wen and M. Gong, *Carbohyd. Poly.*, **74**, 680 (2008).
12. L. Zhao and J. Chang, *J. Sci. Mater: Mater. in Med.*, **15**, 625 (2004).
13. D. Joel Bumgardner et al., US Patent, 0254007 A1 (2007).
14. P. Mathew, N. S. Binulal, S. Soumya, S. V. Nair, T. Furuike, H. Tamura and R. Jayakumar, *Carbohyd. Poly.*, **79**, 281 (2009).
15. B. D. Boyan, et al., US Patent, 5,492,697 (1996).
16. E. Dietrich, H. Oudadesse, A. Lucas-Girot and M. Mami, *J. Biomed. Mater. Res. A*, **88**, 1087 (2008).
17. X. V. Bui, H. Oudadesse, Y. Le Gal, O. Merdrignac-Conanec and G. Cathelineau, *Korean J. Chem. Eng.*, **29**(2), 215 (2012).
18. X. V. Bui, PhD, *Elaboration de biomatériaux verres-substances actives (Zoledronate-Chitosan)*, Order Number 4421, University of Rennes 1, France, 171, 21 November 2011.
19. T. Kokubo, H. Kushitani, S. Sakka, T. Kitsugi and T. Yamamuro, *J. Biomed. Mater. Res.*, **24**, 721 (1990).
20. D. Massiot, F. Fayon, M. Capron, I. King, S. Le Calvé, B. Alonso, J. O. Durand, B. Bujoli, Z. Gan and G. Hoaston, *Magn. Reson. Chem.*, **40**, 70 (2002).
21. M. W. G. Lockyer, D. Holland and R. Dupree, *J. Non. Cryst. Solids*, **188**, 207 (1995).
22. I. Elgayar, A. E. Aliev, A. R. Boccaccini and R. G. Hill, *J. Non. Cryst. Solids*, **351**, 173 (2005).
23. A. Angelopoulou, V. Montouillout, D. Massiot and G. Kordas, *J. Non. Cryst. Solids*, **354**, 333 (2008).
24. Z. R. Hinedi, S. Goldberg, A. C. Chang and J. P. Yesinowski, *J. Colloid Interface Sci.*, **152**, 141 (1992).
25. P. S. Belton, R. K. Harris and P. J. Wilkes, *J. Phys. Chem. Solids*, **49**, 21 (1988).
26. W. P. Aue, A. H. Roufosse, M. J. Glimcher and R. G. Griffin, *Biochem.*, **23**, 6110 (1984).
27. K. S. K. Lin, Y. H. Tseng, Y. Mou, Y. C. Hsu, C. M. Yang and J. C. C. Chan, *Chem. Mater.*, **17**, 4493 (2005).
28. N. G. Philips, Andy Y. YHLo, I. B. Isabel, G. Ana, A. Daniel, S. Bal-

tzar, G. Jekabs, V. R. Maria and E. Mattias, *J. Phys. Chem. C*, **114**, 9345 (2010).
29. A. Diaz, T. Lopez, J. Manjarrez, E. Basaldella, J. M. Martinez-Blanes and J. A. Odriozola, *Acta Biomater.*, **2**, 173 (2006).
30. H. Oudadesse, E. Dietrich, X. V. Bui, Y. Le Gal, P. Pellen and G. Cathelineau, *Appl. Surf. Sci.*, **257**, 8587 (2011).
31. K. J. D. Machenzie and M. E. Smith, *Multinuclear solid-state NMR of inorganic materials*, Cambridge: Pergamon Mater Series (2002).
32. R. Oestrike, W. H. Yang, R. J. Kirkpatrick, R. L. Hervig, A. Navrotsky and B. Montez, *Geochem. Cosmochim Acta*, **51**, 2199 (1987).
33. H. Oudadesse, USTV, October 2011, Rennes, France (2011).
34. O. H. Anderson and K. H. Karlsson, *J. Non. Cryst. Solids*, **129**, 145 (1991).
35. N. Alno, F. Jegoux, P. Pellen-Mussi, S. Tricot, H. Oudadesse, G. Cathelineau, G. De Mello and G. J. Biomed, *Mater. Res. A*, DOI:10.1002/jbm.a.32818.
36. E. Dietrich, PhD, *Syntheses et etudes physic-chimiques de verres bioactifs denses et poreux*, Order Number 3767, University of Rennes 1, France, 205, 17 October 2008.